Colloids and Surfaces A: Physicochem. Eng. Aspects 459 (2014) 142–150

Contents lists available at ScienceDirect

Colloids and Surfaces A: Physicochemical and Engineering Aspects

journal homepage: www.elsevier.com/locate/colsurfa

Immobilization of colloidal particles into sub-100 nm porous structures by electrophoretic methods in aqueous media

K. Kusdianto[a,c], M. Nazli Naim[a,d], Keitaro Sasaki[a], I. Wuled Lenggoro[a,b,*]

[a] Graduate School of Bio-Applications and Systems Engineering, Tokyo University of Agriculture and Engineering, Koganei 184-8588, Tokyo, Japan
[b] Department of Chemical Engineering, Tokyo University of Agriculture and Engineering, Koganei 184-8588, Tokyo, Japan
[c] Department of Chemical Engineering, Institut Teknologi Sepuluh Nopember, Jalan ITS Raya, Surabaya 60111, Indonesia
[d] Department of Process and Food Engineering, Universiti Putra Malaysia, 43400 UPM Serdang, Selangor Darul Ehsan, Malaysia

HIGHLIGHTS

- Electrophoresis of nanoparticles in aqueous media using DC and pulse-DC modes.
- Immobilization of pre-synthesized particles into sub-100 nm porous structures.
- Deposition efficiency of particles inside the pores can be enhanced by pulse-DC mode.
- A removal/detachment test evaluated the "strength" of particle adhesion.

GRAPHICAL ABSTRACT

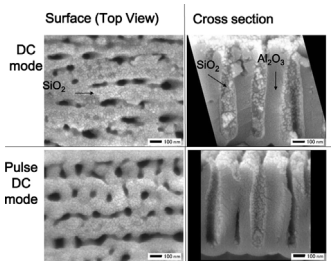

ARTICLE INFO

Article history:
Received 13 March 2014
Received in revised form 19 June 2014
Accepted 23 June 2014
Available online 28 June 2014

Keywords:
Anodic aluminum oxide
Nanoparticle
Electrophoresis
Pulse
Detachment

ABSTRACT

Conventional direct current (DC) and pulse-DC assisted electrophoretic depositions of colloidal particles, with average sizes of 10 and 50 nm, into sub-100 nm scaled pore arrays made from anodized aluminum substrate has been investigated. At the applied voltages lower than the decomposition voltage of water (~1 V), the number concentration of particle deposited on the surface by conventional DC was higher than that of pulse DC. The number of deposited particles increased with increasing pH. Deposition efficiency inside the pores can be enhanced by applying pulse DC. In the case of high (~10 V) applied voltage, no particles were observed inside pores even though pulse DC has been applied. The adhesion strength (removal behavior) of deposition was evaluated by applying a particle detachment simple system based on ultrasonic energy. The particles deposited inside the pores were not detached compared with those of the surface of the substrate.

1. Introduction

Deposition of suspended particles in aqueous media using electrophoretic deposition (EPD) promotes electrokinetic phenomena such as electrophoresis, water hydrolysis and electro-osmosis [1–4]. When the electric field implies a bulk liquid that consists of the suspended particles, a significant motion of charged particles in a suspension or electrophoresis is noticed. In the vicinity of two electrodes, deposition of charged particles onto a substrate surface with an opposite charge occurs. Since then, various techniques to deposit particle materials have been invented [5–11]. However, bubble generation coming from water hydrolysis interrupted the deposition and causes the nm-order particles fail to deposit [5]. Thick film using EPD also contribute to electro-osmosis that could

* Corresponding author at: Tokyo Univ. of Agriculture and Technology, Department of Chemical Engineering, Nakacho 2-24-16, Koganei, Tokyo, Japan.
Tel.:+81 42 388 7987; fax: +81 42 388 7987.
E-mail address: wuled.@cc.tuat.ac.jp (I.W. Lenggoro).

http://dx.doi.org/10.1016/j.colsurfa.2014.06.042
0927-7757/

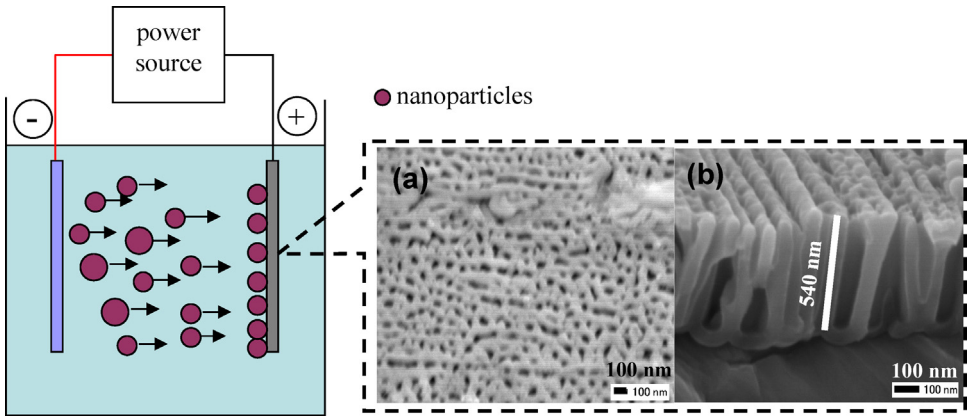

Fig. 1. A schematic diagram of electrophoretic deposition using constant and pulse DC modes (left) and FE-SEM images of aluminum anodizing (right) using H_3PO_4 0.6 M at 50 V for 10 min on (a) surface and (b) cross section area.

damages deposit layer and the surface when long deposition time was conducted [6]. Therefore, controls of certain EPD parameters are very important in order to ensure the deposit are uninterrupted during the deposition process. For examples to prevent the bubble generation, several EPD techniques has been invented such as alternating current (AC) EPD, pulse DC EPD, low voltage deposition and solvent–aqueous mixtures [5–10,12–15].

On the other hand, the unique porous structure of a substrate is widely employed as not only a container (e.g., for catalysts with a high specific surface area), but also for other applications such as membrane filter and hard template for nano-materials [16–19]. Electrophoresis approaches using porous substrates based on anodic aluminium oxide (AAO) [20–22] or graphite [23] had been already reported with using non-aqueous media. In the current work, we demonstrate the immobilization of pre-synthesized nanoparticle (colloidal samples) by EPD technique with conventional-DC and pulse-DC modes onto the porous AAO substrate having pore size of below 100 nm. Several parameters such as pH, applied voltage, and size of colloid were varied in order to evaluate the deposition mechanism. Post-deposition evaluation was also conducted by detachment (removal) of the deposited particles from substrate based on ultrasonic energy.

2. Experimental methods

2.1. Preparation of porous substrate (AAO)

Nanoporous of alumina was formed by electrochemical anodizing of pure aluminum (99.99%) with 0.25 mm diameter and 80 mm length using a laboratory-made anodization cell [24,25]. The plate was used as an anode, and platinum wire with 0.1 mm diameter was used as a cathode. Two electrodes were immerged into 100 ml electrolyte solution, which consisted of 0.6 M phosphoric acid (Wako Pure Chemical Industries, Tokyo) with a distance of 20 mm.

After preliminary experiments using various voltages and times, the anodizing of aluminum was carried out at 50 V and 10 min. The anodic aluminum oxide (AAO) was used as a substrate for deposition and placed as the anode (Fig. 1).

2.2. Particle deposition

Bath media was prepared by diluting SiO_2 colloidal samples (Snowtex types S and 20L, Nissan Chemical Industries, Tokyo) with ultra pure water (Millipore Japan, Tokyo) to be 2 wt%. To simplify the name of colloidal samples, we used "colloid A" and "B" referred to Snowtex S and 20L, respectively. Colloid A and B have a mean diameter of 8–11 and 40–50 nm, respectively. These values are given by the maker. On the other hand, we also measured the particle sizes in liquid phase after a dilution mentioned in Section 2.4.

Each electrode was immerged into the SiO_2 suspension at 298 ± 2 K (Fig. 1). The experimental setup was carried out by varying such conditions as: pH (3 and 7), voltage (1 and 10 V), and colloid size (A and B). All experiments were conducted using constant DC and pulse DC modes. A schematic diagram of constant and pulse DC is depicted in Fig. 2, in which the height represents the magnitude of the applied voltage. In the case of pulse DC mode, it was conducted at the constant voltage mode by applying of a series of DC pulse of an equal amplitude separated by periods of zero voltage. Nitric acid (Wako Pure Chemical Industries) was used for adjusting pH and monitored by a pH probe placed in the bath.

The experimental setup was performed using a laboratory-made built circuit, calibrated with a digital electrometer (Keithley 617, Keithley Instrument Inc., Ohio), and an oscilloscope (TDS 2002B, Textronix Inc., Tokyo) was used to control the pulse current. The frequency of each pulse cycle, 40 Hz, was kept constant for each batch. Pulse time intervals and frequencies were controlled by a field-effect transistor (FET).

2.3. Detachment (removal) of the deposited particles from substrate

After getting the deposited particles on the substrate, the same samples (substrates) were immersed into ultrapure water and placed inside a container made from either glass or poly-propylene resin film. An evaluation of detachment of deposited particles was

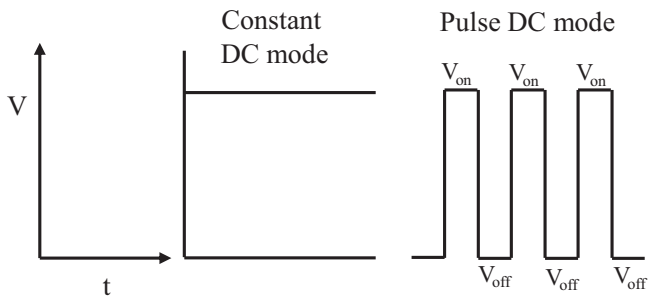

Fig. 2. A schematic diagram of constant DC (left) and pulse DC modes (right).

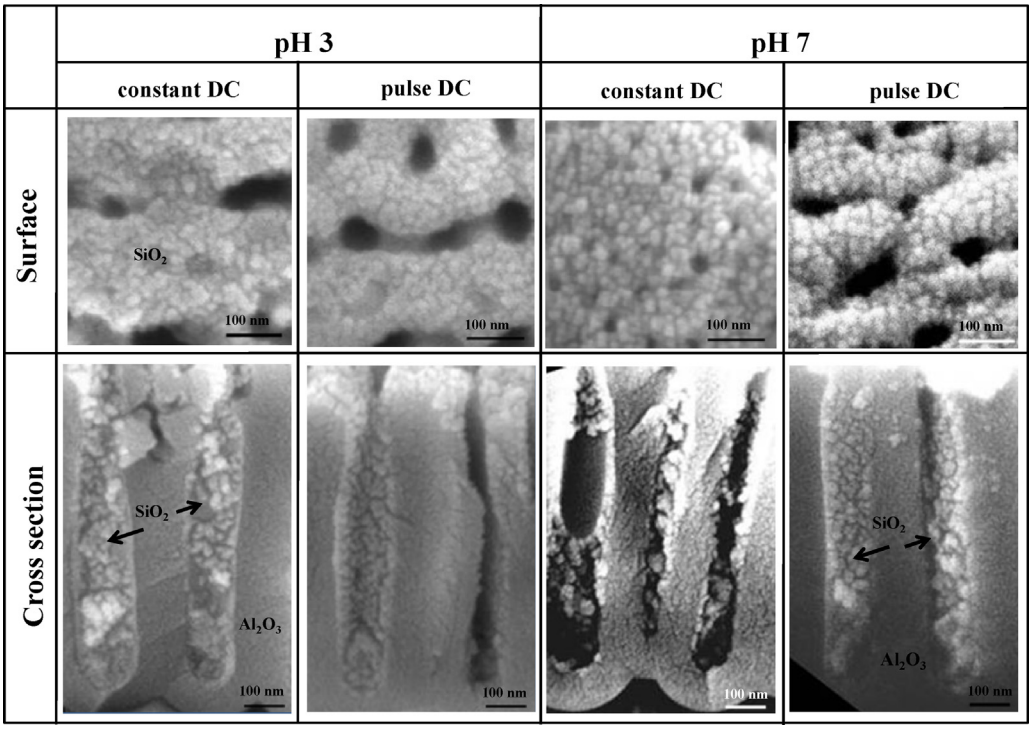

Fig. 3. Deposition of colloid A on the surface and the cross section area using constant DC and pulse DC modes at pH (3 and 7), 1 V, 40 Hz, and 30 min.

performed where the container was placed into ultrasonic bath (UT-105S, Sharp, Tokyo) operated at 35 kHz. The evaluation using a resin film can provide stronger energy comparing to that glass to investigate the bonding strength between the particles and the substrate. Sonication time was varied from 1 to 10 min. The samples prepared by a series of parameter conditions: colloid size (A and B), pH (3), applied voltage (1 V), deposition time (15 min), and frequency (40 Hz).

2.4. Characterization

The pH of suspension was measured by a pH meter (HM-30R, TOA-DKK, Tokyo). Particle-size distributions in the liquid phase were measured by dynamic light scattering (DLS) analysis (HPPS 5001, Malvern Instrument, Worcestershire). The average particle diameters were 10 and 50 nm for colloid A and B, respectively. Size distribution for colloid A was in the range between 6 and 35 nm, while colloid B was a broader range, between 28 and 190 nm. The zeta potential of the sample was measured by an electrophoresis-based zeta potential analyzer (Model 502, Nihon Rufuto, Tokyo) in order to determine the average surface charge available on the surface of the suspended particles.

The samples were put in an oven at 353 K for 2.5 h after EPD and before the analysis. A field emission scanning electron microscope (JSM 6335F JEOL, FE-SEM, Tokyo) was used to observe the AAO on the surface, the cross section view, and the morphology of the deposited particles after experiment. The cross section of the substrate was prepared by cutting of the substrate using a crimping tool. This simple method was used to avoid some effects that might have originated from the argon ion gun and the acceleration voltage from the ion beam cross section polisher.

2.5. Numerical simulation

In addition, the electric field working inside the pore and its vicinity during EPD was also studied using a finite-element based software (COMSOL Multiphysics Ver. 4.3). In this study, only a single pore was investigated as a model, where the boundary conditions were the inlet of aluminum with electrical conductivity of 2.326×10^7 S/m, set 1 V as applied voltage, while the outlet was grounded. The entire system was insulated and the pore material was set as Al_2O_3 with electrical conductivity 35 S/m. Furthermore, the electric field and its potential were estimated using the following equation.

$$J = \sigma \times E + J^e; \quad E = -\nabla V \tag{1}$$

where, J is current density (A/m^2); σ is electrical conductivity (S/m); E is electric field (V/m); J^e is externally generated current density (A/m^2); and V is electric potential (V).

3. Results and discussion

3.1. Morphology of the AAO

A substrate having arrays with sub-100 nm scale pores used for anode was prepared by anodizing of aluminum using phosphoric acid. Phosphoric acid was used as electrolyte because it can increase pore diameter in comparison with other electrolytes, such as sulfuric acid, oxalic acid, and chromic acid, at an equal applied voltage [24]. Formation of pores during an anodizing process is known to depend on the electrolyte type, applied voltage, concentration and temperature [26]. On the other hand, the pore diameter was also increased linearly with voltage [27]. The morphology of the AAO on the surface and cross-section was examined by FE-SEM (Fig. 1), where the average diameter of pores was about 80 nm, whereas the height of the AAO template was estimated to be about 600 nm.

3.2. The effect of pH

The effect of pH on the deposition of particles was investigated by setting pH to be 3 and 7. It was chosen because the average particle size of colloid A (10 nm) measured using DLS at both pH did not

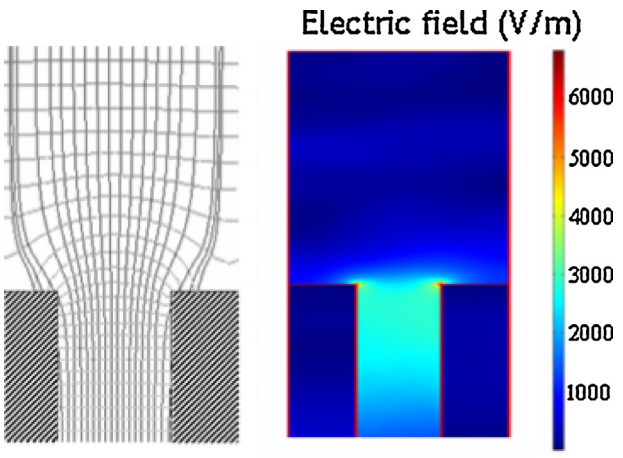

Fig. 4. Results of numerical simulation of electric field pattern around the pore (left) and the contour of electric fields (right).

show a significant difference. Fig. 3 shows the particles deposited on the surface area and pores (cross section) at pH 3 and 7 using the constant DC and pulse DC modes at 1 V, 40 Hz, and 30 min. At both pH values, the amount of particles deposited on the surface (top of the "pillar") by the constant DC mode was higher than that by the pulse DC mode. Particles were continuously attracted to the substrate when the DC mode was applied due to the existence of constant electric fields during the deposition. In contrast, pulse EPD was conducted by applying of a series of DC voltages separated by zero voltage at equal periods (Fig. 2). Initially, the particles were attracted to the substrate when the voltage was applied due to the electrophoretic force. However, the particles were in "stop" position when off-mode was conducted. The electrophoretic force and electroosmosis does not work at the off-mode condition and the suspended particles gather near the substrate without deposition [5]. When the second on-mode was applied, nearby particles were attracted to the substrate by the electrophoretic force. This on/off mechanism was regularly repeated with the same period according to the set voltage.

The amount of particles deposited on the surface at pH 7 was higher than that of pH 3 (Fig. 3). This indicates that the electrophoretic force working at pH 7 was stronger than that at pH 3 because of the higher negative zeta potential at pH 7. The value of the zeta potential at pH 3 (−11 mV) and pH 7 (−28 mV) indicate that the particles are negatively charged in suspension. It is attracted to the positive electrode (AAO) because the driving force is the charge on the particle and the electrophoretic mobility of the particles in the solvent under the influence of an applied electric filed [28]. Therefore, no particles were deposited on the cathode. Moreover, the mobility and the deposition rate of EPD depend on the zeta potential instead of the concentration of suspended particles [29]. The zeta potential decreases with a decrease in pH being affected by the dissociation or ionization behavior of the surface hydroxyl radicals where the zeta potential of the oxides in the aqueous solution shift from negative to positive with decreasing pH [11].

The particles can be incorporated on the pores (between the pillars and the bottoms) for all experimental conditions (Fig. 3). Generally, more particles can be deposited on the pores using the pulse DC comparing with the use of a constant DC mode, as shown in Figs. 3, 5 and 6. This can be attributed to the movement of single/individual particle rather than aggregated particles. Naim et al. found that the pulse DC mode can prevent particle aggregation during electrophoretic deposition [5]. The effect of bubble formation for inhabitation of particles deposited on the pores can be neglected. Because the EPD was carried out at 1 V which is the lower value than decomposition voltage of water. Moreover, the electric fields at the pore wall of AAO can attract negatively charged particles. It was reported that the pore walls of the anodic alumina are positively charged [10]. On the other hand, particle movement occurred because the average particle size (∼10 nm) was smaller enough than the average pore diameter (∼80 nm) so that particles can be incorporated into pores structures of AAO. Kamada et al. reported that the average particles size (∼20 nm) could be inserted into pores with a diameter of 100 nm [10]. However, they could not be positioned into the pores if the particle sizes were 5 nm smaller than the pore diameter. It means that particle sizes should be significantly smaller than the average pore diameter.

A numerical simulation was also performed to study the electric fields working around the pores. The electric fields working during EPD were observed not only on the surface of the substrate but also inside the pore (Fig. 4, left side). This may have caused particles having negative charges can be attracted into the pores due to electrophoretic mobility. Moreover, the highest electric filed working in EPD was observed around the edge of the surface (right side) induces deposition of more particles on the surface than inside the pores. The electric fields that appear in the pores then enhance the attraction force between the substrate and the particles due to the electrokinetic interaction (electrophoretic and electroosmosis). For this reason, particles can be inserted into the pores, but other phenomena also play important roles during EPD, such as aggregated or single (individual) particle movement.

3.3. The effect of particle size

The effect of particle sizes on the final particle structure was studied at pH 3, 40 Hz, 1 V, and 15 min. For both colloid types (Fig. 5), the amount of particles deposited on the surface using constant DC was higher than that of pulse DC. Most of the deposited particles could cover the surface area when constant DC was applied. These results represent the same tendency as the effect of pH on the deposition. As explained in Section 3.2, the electric fields generated by constant DC mode attracted negative charges of particles continuously without any lag compared to pulse DC.

Under the present conditions, colloid A could also be incorporated into the pores using constant or pulse DC (Fig. 5). In contrast to the observation in the preceding subsection, no particles were incorporated into the pores in this case of constant DC mode of colloid B. This indicates that the size difference between the particle and the pore is an important factor in the insertion. Fig. 5 shows that the amount of the deposited particles of colloid A was higher than that of colloid B. Particles having with smaller diameters may deposit more readily than larger particles due to higher mobility and higher surface area [8]. No deposition of colloid B into the pores was probably caused by aggregation of the particles on the surface inhibiting the insertion. Initially, particles remain in suspension without electric fields (off-mode), and then particles were attracted to the electrode as individuals and aggregated after turning on the voltage. By applying continuous voltage, then aggregated particles make clogging in the pore holes then single particles cannot enter the pores. When the colloid B was used, aggregated particle larger than 50 nm were also detected using DLS, where the maximum particle size was about 190 nm. Particle aggregates having similar sizes to pore diameters may cause clogging on the pores.

Even though no particles were deposited inside the pores with constant DC, but sizeable particles were observed in the pores when pulse DC was conducted (Fig. 5). This implies that particles can be introduced by applying pulse DC into the pores due to the faster movement of single particles than that of aggregated particles. This hypothesis is relevant to our previous work, where small cluster or single particles move and deposit faster than aggregate during pulse DC [9]. When the off mode (pulse) was applied, the motion of particles was "stopped" and only Brownian motion was

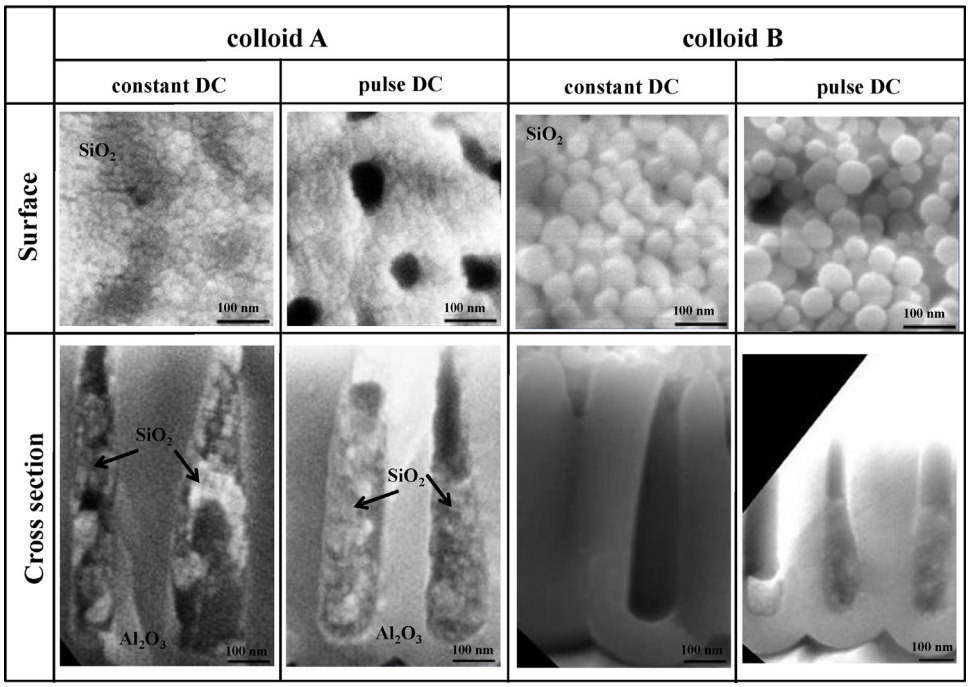

Fig. 5. Deposition of SiO_2 particles on the surface and the cross section area using constant DC and pulse DC modes at various colloid type (colloid A and B), pH 3, 1 V, 40 Hz, and 15 min.

working. After starting the applied voltage, all particles were attracted to the near electrode and single particle that have higher mobility than aggregate particles entered the pores. Additionally, these phenomena may be attributed to electroosmosis, in which as the particles approach the substrate surface, the electroosmosis force interferences within the range of the Deybe length [30,31]. This force bends the initial electrophoretic force, and it drives the incoming particles more strongly to nearby predeposited particles, so that it causes aggregation if the electric field is continued [5]. As the electroosmosis force was stopped at the off-mode condition of the pulse, nearby particles were attracted to the substrate (at second on-mode occurs) with less influence from the electroosmotic force, because the velocity of electrophoresis was higher than that of electroosmosis [1,32,33].

3.4. The effect of applied voltage

Experiments were also carried out by varying voltages (1 and 10 V) at 40 Hz, pH 3, and the deposition time of 5 min using colloid A. Fig. 6 shows that particles were deposited on both surface and pores

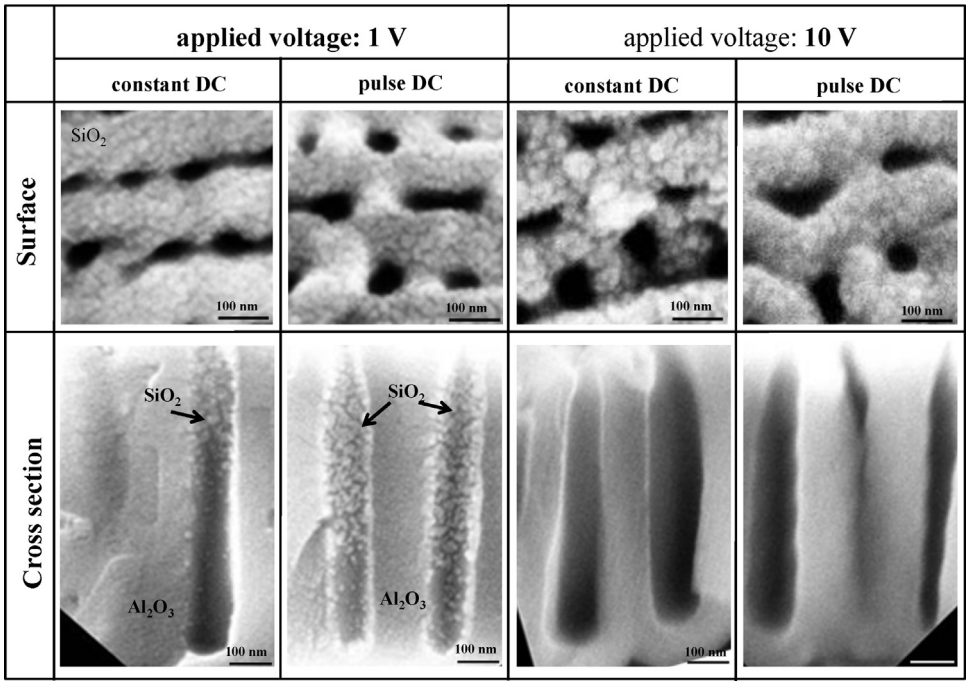

Fig. 6. Deposition of colloid A on the surface and the cross section area using constant and pulse DC modes at 1 and 10 V, pH 3, 40 Hz, colloid S, and 5 min.

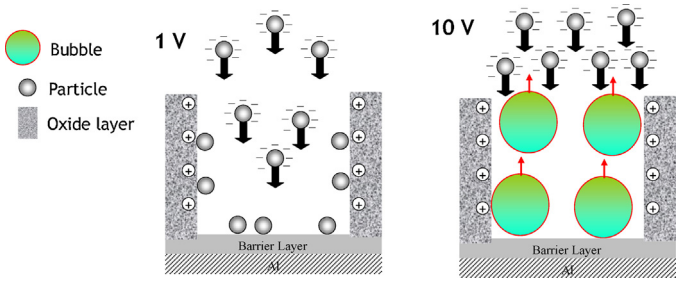

Fig. 7. A schematic illustration of electrophoretic deposition on a porous substrate in the presence of bubbles in different applied voltage.

using either constant or pulse DC modes when the voltage was set at 1 V. The amount of deposited particles on the pores using pulse DC was higher than that using constant DC. As mentioned in Section 3.3, more single particles could be deposited on the substrate by pulse DC than those by constant DC.

Particles were deposited on the surface using of both constant and pulse DC at 10 V (Fig. 6). Unlike in the case of 1 V, no particles were deposited in the pores even when the pulse DC was applied. This condition may be caused by bubble formation at the electrode surface that disturbed the migration of particles toward the pores. Since the decomposition voltage of water (1.23 V at 298 K) is much lower than 10 V, bubble formation (probably with a critical size) cannot be avoided during deposition [6]. Water electrolysis

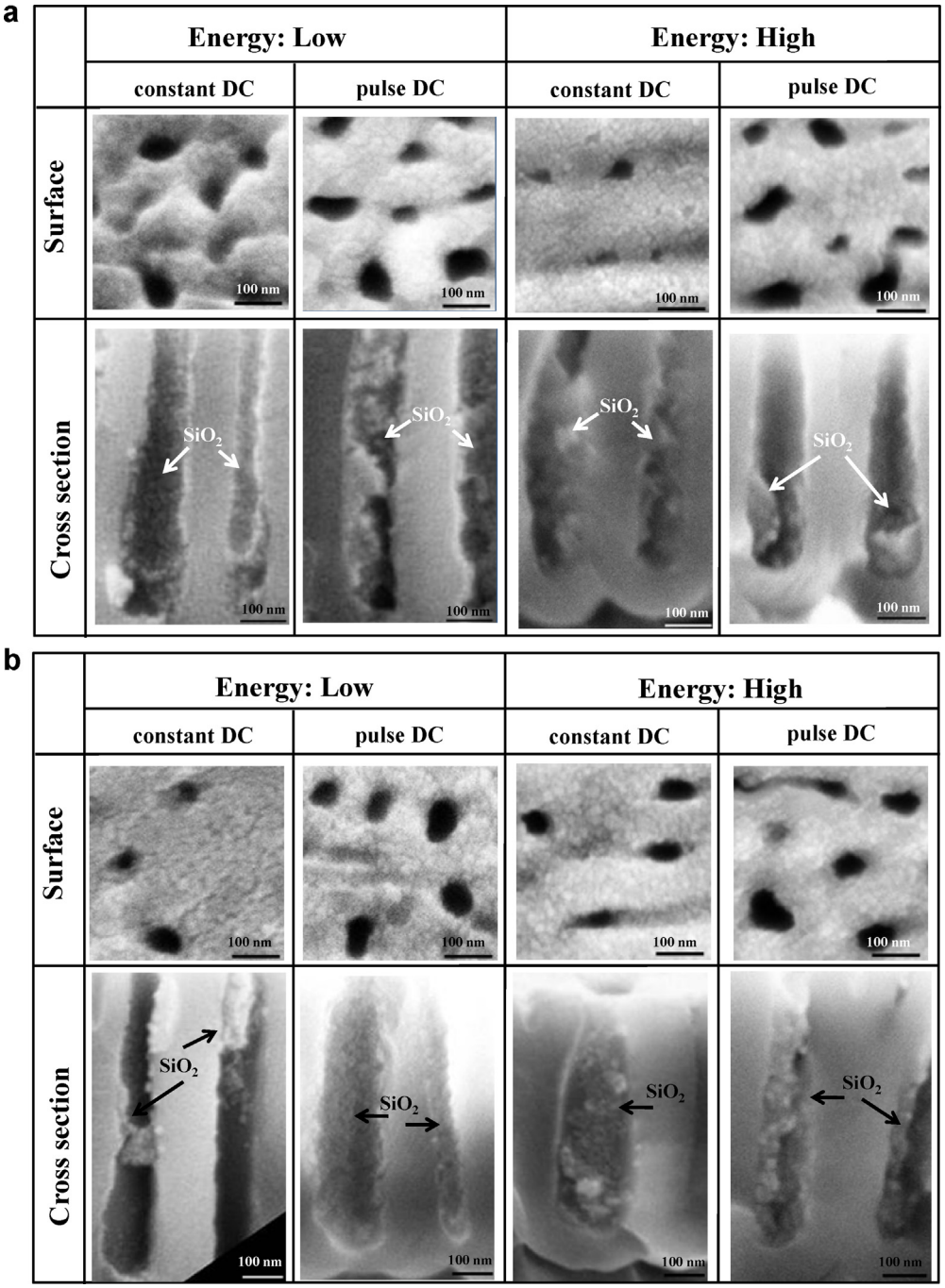

Fig. 8. Detachment of the deposited particles using different "energy" in ultrasonic wave at 35 kHz for (a) 1 min, (b) 10 min. The samples before sonication were prepared by EPD at conditions of pH 3, 1 V, 10 min, 40 Hz and colloid A.

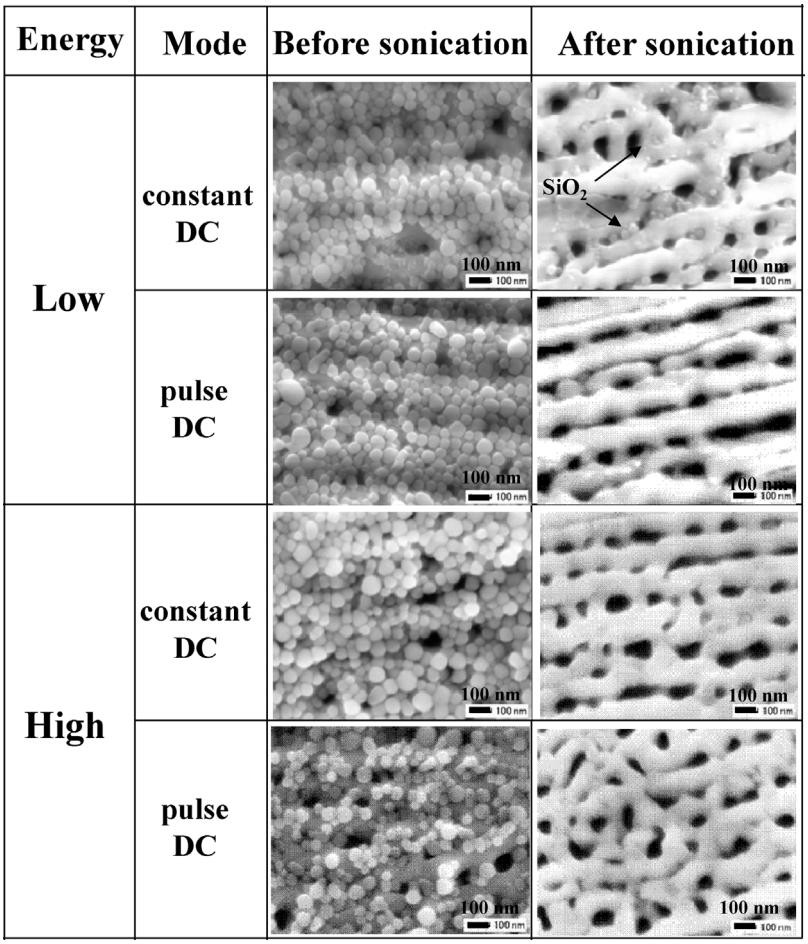

Fig. 9. Detachment of the deposited particles using different "energy" in an ultrasonic bath at 35 kHz for 30 min. The samples before sonication were prepared by EPD at pH 3, 1 V, 15 min, 40 Hz and colloid B.

generates the formation of H_2 and O_2 at the cathode and anode where the volume of H_2 gas produced is twice that of O_2 gas. Though H_2 gas produced has a larger volume than that of O_2 gas in this system, the solubility of hydrogen (1617.6 mg/L) in water at 298 K and 10^5 Pa is higher than that of oxygen (43.3 mg/L) [7]. The lower solubility of oxygen causes more bubbles suspended or trapped inside the pores and then they interfere insertion of particles into the pores. The applied voltage at 10 V will generate stronger electric field than 1 V, by which the electrophoretic mobility of particles is also enhanced. Nevertheless, application of high voltage will generate more bubbles at electrode due to stronger water electrolysis.

It was reported that the bubble formation could be started from 30 nm, in an electrolysis of water [34]. The bubbles then grow and make aggregation forming the micro-meter sized bubble. Svetovoy et al. investigated that the microbubbles (20–50 μm) were formed due to aggregation of nanobubble (200 nm) in 20–50 μs [35]. In the present study, we assume that the bubbles can be formed inside the sub-100 nm porous structures. The pressure within these bubbles will be increased, because it is linearly proportional with bubble size. The increasing pressure may enhance solubility of bubble in liquid and make aggregation. The aggregated bubble will inhibit the incoming particle to be deposited on the electrode. The smaller particles could not be deposit on the surface, because they were not able to overcome the resistance of bubbles. However, aggregated (larger) particles may be possible to overcome the resistance due to higher momentum.

Naim et al. also investigated that the morphology of deposited particles on the surface showed more compact when applying pulse DC mode [9]. The crack structure was also observed on the interface between electrode and deposited particle after applying a constant DC mode. These phenomena might be attributed due to bubble formation, and related to the evolution of hydrogen and oxygen gas in electrodes. By applying pulse DC mode, the bubble could be suppressed and morphology of the deposited particles were possible to be "smoother" [7].

In the case of pulse DC, some bubbles were still in the pores. This is probably caused by the time limitation of bubbles to escape from the pores due to the lower solubility in water. Accumulation of bubbles inside the pores will enhance the pressure at the bottom of pores and overcomes the force (or momentum) for introducing of particles. In order to solve this problem, it is necessary to optimize the pattern of pulse DC by extending the pulse width to allow enough time of bubbles to escape from the pores then particles can be introduced into pores.

The illustration of competition between bubbles formation and insertion mechanism of particles inside the pore in different applied voltage is depicted in Fig. 7. Particles with negative charges tend to deposit in the anode when the electric field is applied. In the case of applied voltage at 1 V, the bubbles were not produced because theoretically this voltage is less than the decomposition voltage of water due to electrolysis. The mechanism of particle deposition in the surface and pore depend on the electrical mobility of the particles, and their movement as

aggregate or single/individual particle. If the applied voltage is higher than the decomposition voltage of water, the bubble formation will affect to particle deposition. In general, the particles movement of EPD is caused by electrokinetic phenomena (electrophoresis and electroosmosis). Negatively charged particles can be inserted into the pores when electrophoretic mobility can overcome the forces derived from bubble formation. Since the bubbles are produced by water electrolysis, their amount is increased with the applied voltage. If many bubbles are trapped inside the pores, electrophoretic and electroosmosis should be suppressed by the forces caused by accumulation of bubbles. Despite the positive charge of aluminum oxide, however, the electrostatic force induced by this layer is not strong enough to attract negatively charged particles.

To provide sufficient time for bubbles to escape from the pores, the pulse width should be extended, and addition of a chemical into the suspension may be useful to obtain a bubble-free system during the deposition. Hence hydroquinone was added to the alkaline aqueous solution during EPD in order to generate a bubble free area on the anode substrate, oxygen gas was believed to be consumed by the chemical oxidation of hydroquinone to quinine at high pH in alkaline solution [2].

3.5. Evaluation of the deposited particle structures

Fig. 8(a) and (b) shows the morphology on the surface and the cross section area after sonication with different "energy levels" in 1 and 10 min, respectively. By comparison of the surface morphologies before (Fig. 5, upper site) and after (Fig. 8) sonication, it can be generally observed that most of the particles on the surface were detached. Particles with smaller sizes observed on the surface (Fig. 8) were also observed in the pores. Most of these particles could not be detached from the pores because the ultrasonic force reaching inside the pores was weaker than those on the surface. On the other hand, incorporation of the particles and the surface may have been caused by the adhesion force among them [36]. The detachment of particles from the surface was mainly induced by the mechanical effect of ultrasound caused by cavitation of bubbles [37].

In order to investigate more detail about particles detachment mechanism, the results using colloid B having larger particles (~50 nm) was also carried out. Fig. 9 shows the surface structure of particle before and after sonication. Most of particles can be detached from surface. However, some particles are observed when lower ultrasonic energy (using glass container) was applied especially for constant DC mode. From an image analysis, the detachment efficiency was calculated by comparing the area of the particles detached from the surface versus the area (initial condition) before particle detachment. For colloid B, for instance, it was found that the detachment efficiency by high energy was higher (99.3%) than that of low energy (94.7%). It indicates that more particles could be detached from the surface when the high energy was conducted.

This result indicates that when constant DC was applied, the electrostatic force between particles and AAO substrate was higher than that of pulse DC, then causing the stronger attraction force among them. On other hand, the higher negatively charges of particles may contribute for enhancing the adhesion force between particles and surface because the stronger adhesion of particles to substrate was observed at pH values away from isoelectric point (IEP) [6]. It is well known that at the near IEP, the van der Waals attractive forces between particles are strong due to absence of electrostatic force. In overall, the deposited particles inside the pores was relatively difficult to detach (using ultrasonic wave) and then it may be useful for further applications, such as photocatalysis materials and other devices.

4. Conclusions

Electrophoretic deposition (EPD) of particles onto a sub-100 nm scaled pore arrays made from anodized aluminum has been investigated. By applying voltage lower than the decomposition voltage of water, the number of deposited particles on the surface using constant DC was found to be higher than that of pulse DC due to continuously electric fields attracting particles. The increase in the number of particles deposited on the substrate increased with an increase in pH can be ascribed to the stronger electrophoretic mobility of particles caused by the higher negative value of the zeta potential.

Particles having different sizes (below 100 nm) can be deposited on the surface by conducting EPD using constant DC, however, no larger particles can be inserted into the pores. However, the particles can be inserted into pores by using pulse DC, probably because the pulse DC allows single particles to move faster than aggregate particles. Moreover, electroosmosis was "stopped" when the "off" mode at pulse DC was applied. Then the particles move to the substrate with less influence of electroosmosis while the next "on" mode was conducted. Thus these phenomena have led to easier insertion of particles into the pores.

At higher (10 V) voltage, particles were only deposited on the surface and no particles were detected in the pores even by application of pulse DC. At voltage higher than the decomposition voltage of water, more bubbles generated in the pores tend to increase the pressure inside pores. This pressure will interfere migration of particles entering the pores. Particles will be inserted into pores if the particles forces (electrophoretic and electroosmosis) can overcome other forces or pressures derived from bubble formation.

In the experiments of particles detachment, the number of detached particles from surface was higher when higher ultrasonic energy was used comparing to that of lower energy and most of particles could not be detached from the pores.

Acknowledgements

The authors are grateful to Drs. H. Kamiya, M. Iijima, M. Kuwata and M. Tsukada for supports, Dr. K. Kuchitsu for English-editing, Mr. Y. Yamada and M. Gen for assistance in simulation. This study was supported in part by Special Condition Funds for Promoting Science and Technology from the Japan Science and Technology Agency (JST), Grant-in-Aid for Scientific Research from the Japan Society for the Promotion of Science (JSPS: 26420761, 23246132, 23560904) and Grants-in-Aid for Scientific Research on Innovative Areas (ASEPH) from the Ministry of Education, Culture, Sports, Science, and Technology. One of the authors' (K. Kusdianto) Doctoral Program Scholarship is supported by Ministry of Education and Culture, Republic of Indonesia.

References

[1] T. Palberg, H. Versmold, Electrophoretic–electroosmotic light-scattering, J. Phys. Chem. 93 (1989) 5296–5301.
[2] O. Sakurada, K. Suzuki, T. Miura, M. Hashiba, Bubble-free electrophoretic deposition of aqueous zirconia suspensions with hydroquinone, J. Mater. Sci. 39 (2004) 1845–1847.
[3] T. Uchikoshi, K. Ozawa, B.D. Hatton, Y. Sakka, Dense, bubble-free ceramic deposits from aqueous suspensions by electrophoretic deposition, J. Mater. Res. 16 (2001) 321–324.
[4] A.V. Delgado, F. Gonzalez-Caballero, R.J. Hunter, L.K. Koopal, J. Lyklema, Measurement and interpretation of electrokinetic phenomena, J. Colloid Interface Sci. 309 (2007) 194–224.
[5] M.N. Naim, M. Iijima, K. Sasaki, M. Kuwata, H. Kamiya, I.W. Lenggoro, Electrical-driven disaggregation of the two-dimensional assembly of colloidal polymer particles under pulse DC charging, Adv. Powder Technol. 21 (2010) 534–541.
[6] L. Besra, T. Uchikoshi, T.S. Suzuki, Y. Sakka, Bubble-free aqueous electrophoretic deposition (EPD) by pulse-potential application, J. Am. Ceram. Soc. 91 (2008) 3154–3159.
[7] L. Besra, T. Uchikoshi, T.S. Suzuki, Y. Sakka, Application of constant current pulse to suppress bubble incorporation and control deposit morphology

during aqueous electrophoretic deposition (EPD), J. Eur. Ceram. Soc. 29 (2009) 1837–1845.
[8] M.N. Naim, M. Kuwata, H. Kamiya, I.W. Lenggoro, Deposition of TiO_2 nanoparticles in surfactant-containing aqueous suspension by a pulsed DC charging-mode electrophoresis, J. Ceram. Soc. Jpn. 117 (2009) 127–132.
[9] M.N. Naim, M. Iijima, H. Kamiya, I.W. Lenggoro, Electrophoretic packing structure from aqueous nanoparticle suspension in pulse DC charging, Colloids Surf., A: Physicochem. Eng. Aspects 360 (2010) 13–19.
[10] K. Kamada, H. Fukuda, K. Maehara, Y. Yoshida, M. Nakai, S. Hasuo, Y. Matsumoto, Insertion of SiO_2 nanoparticles into pores of anodized aluminum by electrophoretic deposition in aqueous system, Electrochem. Solid State Lett. 7 (2004) B25–B28.
[11] K. Kamada, M. Tokutomi, N. Enomoto, J. Hojo, Incorporation of oxide nanoparticles into barrier-type alumina film via anodic oxidation combined with electrophoretic deposition, J. Mater. Chem. 15 (2005) 3388–3394.
[12] A. Chavez-Valdez, M. Herrmann, A.R. Boccaccini, Alternating current electrophoretic deposition (EPD) of TiO_2 nanoparticles in aqueous suspensions, J. Colloid Interface Sci. 375 (2012) 102–105.
[13] S. Lebrette, C. Pagnoux, P. Abelard, Stability of aqueous TiO_2 suspensions: influence of ethanol, J. Colloid Interface Sci. 280 (2004) 400–408.
[14] S. Lebrette, C. Pagnoux, P. Abelard, Fabrication of titania dense layers by electrophoretic deposition in aqueous media, J. Eur. Ceram. Soc. 26 (2006) 2727–2734.
[15] M.J. Santillan, N.E. Quaranta, A.R. Boccaccini, Titania and titania–silver nanocomposite coatings grown by electrophoretic deposition from aqueous suspensions, Surf. Coat. Technol. 205 (2010) 2562–2571.
[16] Y. Matsumoto, Y. Ishikawa, M. Nishida, S. Ii, A new electrochemical method to prepare mesoporous titanium(IV) oxide photocatalyst fixed on alumite substrate, J. Phys. Chem. B 104 (2000) 4204–4209.
[17] T. Kyotani, W.H. Xu, Y. Yokoyama, J. Inahara, H. Touhara, A. Tomita, Chemical modification of carbon-coated anodic alumina films and their application to membrane filter, J. Membr. Sci. 196 (2002) 231–239.
[18] S.J. Limmer, G.Z. Cao, Sol–gel electrophoretic deposition for the growth of oxide nanorods, Adv. Mater. 15 (2003) 427–431.
[19] T.E. Bogart, S. Dey, K.K. Lew, S.E. Mohney, J.M. Redwing, Diameter-controlled synthesis of silicon nanowires using nanoporous alumina membranes, Adv. Mater. 17 (2005) 114–117.
[20] B. Fori, P.L. Taberna, L. Arurault, J.-P. Bonino, C. Gazeau, P. Bares, Electrophoretic impregnation of porous anodic aluminum oxide film by silica nanoparticles, Colloids Surf., A: Physicochem. Eng. Aspects 415 (2012) 187–194.
[21] B. Fori, P.L. Taberna, L. Arurault, J.P. Bonin, Decisive influence of colloidal suspension conductivity during electrophoretic impregnation of porous anodic film supported on 1050 aluminium substrate, J. Colloid Interface Sci. 413 (2014) 31–36.
[22] D. Zhang, G. Dong, Y. Chen, Q. Zeng, Electrophoretic deposition of PTFE particles on porous anodic aluminum oxide film and its tribological properties, Appl. Surf. Sci. 290 (2014) 466–474.
[23] S. Haber, Deep electrophoretic penetration and deposition of ceramic particles inside impermeable porous substrates, J. Colloid Interface Sci. 179 (1996) 380–390.
[24] S. Ono, N. Masuko, Evaluation of pore diameter of anodic porous films formed on aluminum, Surf. Coat. Technol. 169 (2003) 139–142.
[25] H. Masuda, K. Yada, A. Osaka, Self-ordering of cell configuration of anodic porous alumina with large-size pores in phosphoric acid solution, Jpn. J. Appl. Phys., 2: Lett. 37 (1998) L1340–L1342.
[26] M.P. Proenca, C.T. Sousa, D.C. Leitao, J. Ventura, J.B. Sousa, J.P. Araujo, Nanopore formation and growth in phosphoric acid Al anodization, J. Non-Cryst. Solids 354 (2008) 5238–5240.
[27] A.P. Li, F. Muller, A. Birner, K. Nielsch, U. Gosele, Hexagonal pore arrays with a 50–420 nm interpore distance formed by self-organization in anodic alumina, J. Appl. Phys. 84 (1998) 6023–6026.
[28] P.M. Biesheuvel, H. Verweij, Theory of cast formation in electrophoretic deposition, J. Am. Ceram. Soc. 82 (1999) 1451–1455.
[29] Y. Solomentsev, S.A. Guelcher, M. Bevan, J.L. Anderson, Aggregation dynamics for two particles during electrophoretic deposition under steady fields, Langmuir 16 (2000) 9208–9216.
[30] S. Ghosal, Fluid mechanics of electroosmotic flow and its effect on band broadening in capillary electrophoresis, Electrophoresis 25 (2004) 214–228.
[31] H. Ohshima, Electrophoretic mobility of a spherical colloidal particle in a salt-free medium, J. Colloid Interface Sci. 248 (2002) 499–503.
[32] H. Ohshima, Electroosmotic velocity in fibrous porous media, J. Colloid Interface Sci. 210 (1999) 397–399.
[33] L. Besra, M. Liu, A review on fundamentals and applications of electrophoretic deposition (EPD), Prog. Mater. Sci. 52 (2007) 1–61.
[34] K. Kikuchi, A. Ioka, T. Oku, Y. Tanaka, Y. Saihara, Z. Ogumi, Concentration determination of oxygen nanobubbles in electrolyzed water, J. Colloid Interface Sci. 329 (2009) 306–309.
[35] V.B. Svetovoy, R.G.P. Sanders, M.C. Elwenspoek, Transient nanobubbles in short-time electrolysis, J. Phys. Chem.: Condens. Matter 25 (2013) 184002.
[36] J.N. Ding, X.F. Wang, N.Y. Yuan, C.L. Li, Y.Y. Zhu, B. Kan, The influence of substrate on the adhesion behaviors of atomic layer deposited aluminum oxide films, Surf. Coat. Technol. 205 (2011) 2846–2851.
[37] L.H. Thompson, L.K. Doraiswamy, Sonochemistry: science and engineering, Ind. Eng. Chem. Res. 38 (1999) 1215–1249.